Optimal Continuous Control for Remote Orbital Capture

B.A. Conway*
University of Illinois at Urbana-Champaign, Urbana, Illinois
and
J.W. Widhalm†
Air Force Institute of Technology, Wright-Patterson Air Force Base, Ohio

Optimal control histories are presented for the problem of detumbling (passivating) a satellite. It is proposed that this be done remotely by a robot spacecraft, sometimes referred to as a teleoperator or orbital maneuvering vehicle, in preparation for the return of both vehicles to low-Earth orbit. The dynamics of the coupled two-body system are described with equations of motion derived from an Eulerian formulation (the Hooker-Margulies equations). Two degrees of rotational freedom and one of translation are allowed at the joint that connects the orbital maneuvering vehicle and target spacecraft. The initial condition of the target satellite is free spin and precession. Representative masses and inertias are assumed for both bodies. Application of optimal control theory results in a nonsingular, two-point-boundary-value problem that is solved numerically for the controls, which are principally the external (thruster) and internal (joint) torques to be applied by the orbital maneuvering vehicle. Control histories and vehicle motion are found for both constrained and unconstrained fixed-time optimization. Constraint forces and torques at the joint are determined.

Nomenclature

F_λ = total exernal force on body λ
F'_λ = nongravitational external force on body λ
$F^H_{\lambda j}$ = interaction force on body λ transmitted through joint j
$\hat{g}_i$ = unit vector along rotation axis of joint
J_λ = the set of joints on body λ
1 = unit dyadic
m = total mass
m_λ = mass of body λ
r = number of rotational degrees of freedom
T_λ = total external torque on body λ
T'_λ = nongravitational external torque on body λ
$T^C_{\lambda j}$ = gimbal constraint torque on body λ at joint j
$T^H_{\lambda j}$ = torque on body λ transmitted through joint j
$T^{SD}_{\lambda j}$ = spring-damper torque on body λ at joint j
γ = planet's gravitational constant
γ_i = angle of rotation about axis $\hat{g}_i$
ρ = planetocentric position vector of satellite composite c.m.
$\hat{\rho}$ = unit vector in direction of ρ
ρ_λ = planetocentric position vector of c.m. of body λ
Φ_λ = inertia dyadic of body λ about center of mass
ω_λ = angular velocity of body λ
ω_0 = angular velocity of the reference body

Introduction

THE detumbling or "passivation" of a satellite is required before in-orbit servicing of the satellite or retrieval may be done. The first attempt at in-orbit satellite repair occurred in April 1984 when the Solar Maximum spacecraft was captured, repaired, and returned to service in low orbit. The difficulties encountered clearly demonstrated the complexity of the detumbling problem, even though the satellite had very small angular rates. Many, perhaps most, of the satellites which could benefit from servicing or retrieval are in orbits too distant for the space shuttle to reach. An independent or remotely-operated spacecraft, sometimes referred to as a teleoperator or orbital maneuvering vehicle (OMV), is required for such missions.

The OMV would need to rendezvous and dock with the target satellite and then apply forces and torques to the target so as to remove any relative motion. This relative motion is primarily that of the target, particularly if the target satellite is spin-stabilized or has experienced a failure of its attitude control system. Afterward, attitude maneuvers of the coupled system would be performed to orient the vehicle for return to low-Earth orbit. Only the detumbling problem will be described here; research on other aspects of the problem is in progress.

Work began on the problem of remote orbital capture in the early 1970s. Efforts to define the concept and requirements of teleoperator spacecraft were made by Onega and Clingman[1] and by Smith and DeRocher.[2] At the same time the dynamics and control of remote orbital capture began to be considered. Faile et al.[3] analyzed the response of a target spacecraft to torques applied by an OMV which had completed a rendezvous and docking with the target spacecraft. They assumed that the OMV was absolutely stable and ignored the problem of controlling the response of the OMV in applying torques to the target. Kaplan and Nadkarni[4] went farther by proposing an OMV with an articulating arm capable of four degrees of rotational freedom relative to the OMV. A grappling device on the arm was envisioned that could be driven to null its motion relative to the target for docking. The dynamic response of this system to internal torques was analyzed under two critical assumptions. First, articulating counter masses were available to balance dynamically the mass of the articulating arm. Second, the mass of the OMV was large relative to that of the target. While simplifying the dynamic analysis, these assumptions would require the OMV to be very massive and have a very complex control system for the articulating arm and counter masses.

In Ref. 5, a capture problem is formulated in which a 1000 kg target spacecraft is to be retrieved from geosynchronous orbit to low Earth orbit. The OMV for this mission is assumed to use conventional propulsion and to be cylindrical in shape for

Received Oct. 12, 1984; revision received June 20, 1985.

*Assistant Professor, Department of Aeronautical and Astronautical Engineering. Member AIAA.
†Assistant Professor and Lt. Col. USAF. Member AIAA.

Table 1 Spacecraft mass properties

	Mass	I_1	I_2	I_3
Target spacecraft	1000 kg	1000 kg-m^2	1000 kg-m^2	1100 kg-m^2
Retriever spacecraft (OMV)	4500 kg	6400 kg-m^2	6400 kg-m^2	11800 kg-m^2

transport in the Shuttle cargo bay. The mass properties of the target spacecraft and the OMV are given in Table 1. The target spacecraft is assumed to be symmetric about one axis, so that the problem of capturing it from a torque-free steady state of spin and precession can be considered. As shown in Fig. 1, the OMV (body 0) they propose is joined to the target (body 1) through a two degrees of freedom ball and socket joint with a grappling device. An Eulerian derivation of the equations of motion of the two-body system is developed from the general n-body equations given by Hooker and Margulies[6] and Hooker.[7] System response to passivation torques at the joint and external thruster torques on the OMV is analyzed by integrating the equations of motion with a set of Euler angle kinematical equations for the OMV. Since the OMV is not considered absolutely stable, as in the previous work, the simple torque schemes applied did not yield a satisfactory passivation method as evidenced by the propagation of the system orientation and angular rates. This was expected, and Conway et al.[5] concluded that active control of internal and external torques is requried for a satisfactory capture.

This paper is a continuation of the work in Ref. 5 and introduces a translational degree of freedom in the joint on the OMV, formulates the capture problem as a nonsingular two-point-boundary value-problem (TPBVP) using optimal control theory, and solves the TPBVP by a numerical method to yield the continuous, optimal, open-loop passivation controls. Constraints are imposed on the controls in various ways to simplify the control system. To size the structural requirements of the joint on the OMV and the connecting device to the target, the constraint force and torque on the joint is solved for. The component of the constraint force in the direction of joint motion gives the control requirement to move the joint during capture. The results show that detumbling of the target can be accomplished with control torques of very reasonable magnitude. Furthermore, the constraint force and torque are seen to impose only very modest loads on the system.

Method of Capture

All the previous researchers employ the same basic concept for capturing a target spacecraft. An orbital maneuvering vehicle (OMV) or teleoperator maneuvers to an appropriate position near the target. The OMV then drives itself and/or its grappling device to a state of zero relative motion with respect to the target. This allows docking to occur without disturbing the motion of the two bodies. Passivation is effected by applying torques through the grappling device to drive the target to a state of rest relative to the OMV while, in some way, controlling the motion of the OMV.

The method proposed for capture may be described with reference to Fig. 1. In this figure two body-fixed reference frames, having origins at the centers of mass of each body, are shown. The e basis vectors lie along the axes of the frame fixed in body O (the OMV) and the n basis vectors lie along the axes of the body 1 (target) fixed reference frame. For capture, the initial spin rate, $\dot{\psi}$, of the OMV is made equal to the initial precession rate of the target. The initial angular momentum vectors of the OMV and the target are parallel to the $\hat{e}_3$ axis and have the same sign. The center of mass of the target is initially on the $\hat{e}_3$ axis. The joint position on the surface of the OMV is determined by the initial cone angle γ_1 and the distance in the $\hat{n}_3$ direction from the center of mass of the target to the surface of the OMV. The initial value of $\dot{\psi}$ is determined by the initial values of γ_1 and $\dot{\gamma}_2$ for steady spin and precession.[8]

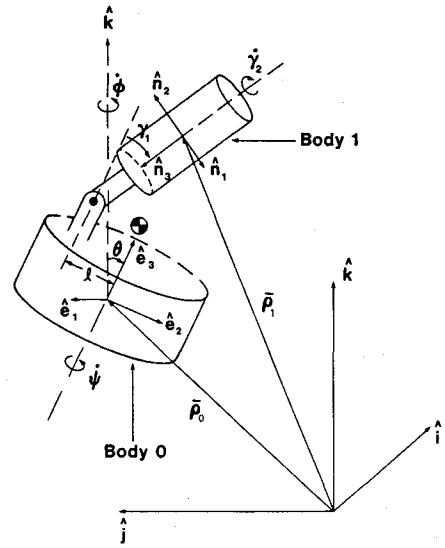

Fig. 1 Spacecraft configuration.

From this stable configuration, torques and forces are applied at the joint by the action of thrusters aboard the OMV to detumble the system. It is proposed that the joint be capable of translation along the surface of the OMV. This has several benefits. If the cone angle γ_1 of the target is not known prior to rendezvous the joint could not be prepositioned. In addition, allowing the joint to return during detumbling to the center of the OMV (the $\hat{e}_3$ axis) would allow the final configuration of the system to be spin stabilized.

Equations of Motion

Several methods are available to formulate equations for the attitude motion of multibody systems. An Eulerian approach is chosen here because then forces and torques appear explicitly. Conway and Widhalm[9] have modified the Hooker and Margulies[6] derivation of the equations of motion to account for translational motion of the joints with respect to the bodies they connect. Their main result, specialized to the case of the two bodies shown in Fig. 1, becomes

$$\begin{bmatrix} a_{00} & a_{01} & a_{02} \\ a_{10} & a_{11} & a_{12} \\ a_{20} & a_{21} & a_{22} \end{bmatrix} \begin{bmatrix} \dot{\omega}_0 \\ -\ddot{\gamma}_1 \\ \ddot{\gamma}_2 \end{bmatrix} = \begin{bmatrix} E_0^* + E_1^* - m_1 \mathcal{L}_{01} \times [\ddot{D}_{01}^R + 2\omega_0 \times \dot{D}_{01}^R] \\ + D_{10} \times m[\ddot{D}_{01}^R + 2\omega_0 \times \dot{D}_{01}^R] \\ \hat{g}_1 \cdot (E_1^* + D_{10} \times m[\ddot{D}_{01}^R + 2\omega_0 \times \dot{D}_{01}^R]) \\ \hat{g}_2 \cdot (E_1^* + D_{10} \times m[\ddot{D}_{01}^R + 2\omega_0 \times \dot{D}_{01}^R]) \end{bmatrix} \tag{1}$$

The $[a]$ matrix is determined by the system masses and configuration,

$$a_{00} = \sum_{\lambda} \sum_{\mu} \phi_{\lambda\mu}, \text{ a dyadic, } 3 \times 3$$

$$a_{0k} = \sum_{\lambda}\sum_{\mu} \epsilon_{k\mu}\Phi_{\lambda\mu}\cdot\hat{g}_k, \text{ a vector, } 3\times 1,$$

$$a_{i0} = \hat{g}_i\cdot\sum_{\lambda}\sum_{\mu}\epsilon_{i\lambda}\Phi_{\lambda\mu}, \text{ a vector, } 1\times 3,$$

$$a_{ik} = \hat{g}_i\cdot\sum_{\lambda}\sum_{\mu}\epsilon_{i\lambda}\epsilon_{k\mu}\Phi_{\lambda\mu}\cdot\hat{g}_k, \text{ a scalar} \tag{2}$$

where

$\epsilon_{i\mu}=1$, if $\hat{g}_i$ belongs to a joint anywhere on the chain of bodies connecting body μ and the reference body

$=0$, otherwise (e.g, if $\mu=0$)

$$\Phi_{\lambda\lambda} = \Phi_\lambda + m_\lambda(D_\lambda^2 1 - D_\lambda D_\lambda) + \sum_{\mu\neq\lambda} m_\mu(D_{\lambda\mu}^2 1 - D_{\lambda\mu}D_{\lambda\mu}) \tag{3}$$

$$\Phi_{\lambda\mu}(\mu\neq\lambda) = -m(D_{\mu\lambda}\cdot D_{\lambda\mu}1 - D_{\mu\lambda}D_{\lambda\mu}) \tag{4}$$

$$D_\lambda = -\sum_{\mu\neq\lambda} m_\mu m^{-1}\mathcal{L}_{\lambda\mu} \tag{5}$$

$$D_{\lambda\mu} = D_\lambda + \mathcal{L}_{\lambda\mu} \tag{6}$$

and $\mathcal{L}_{\mu\lambda}$ is the vector from the center of mass of body λ to the joint leading to body μ. E_λ^* is determined by

$$E_\lambda^* = E_\lambda - \sum_{\mu}\Phi_{\lambda\mu}\cdot\sum_{k}\epsilon_{k\mu}\dot{\gamma}_k\hat{\boldsymbol{g}}_k \tag{7}$$

where

$$E_\lambda = 3\gamma\rho^{-3}\hat{\rho}\times\Phi_{\lambda\lambda}\cdot\hat{\rho} - \omega_\lambda$$
$$\times\Phi_{\lambda\lambda}\cdot\omega_\lambda + T_\lambda' + \sum_{j\epsilon J_\lambda} T_{\lambda j}^{SD} + D_\lambda\times F_\lambda' + \sum_{\mu\neq\lambda} D_{\lambda\mu}$$
$$\times\{F_\mu' + m\omega_\mu\times(\omega_\mu\times D_{\mu\lambda}) + m\gamma\rho^{-3}(1-3\hat{\rho}\hat{\rho})\cdot D_{\mu\lambda}\} \tag{8}$$

In Eq. (1), $\omega_0=\omega_{01}\hat{e}_1+\omega_{02}\hat{e}_2+\omega_{03}\hat{e}_3$, γ_1 and γ_2 are angles of rotational freedom of the joint about gimbal axis $\hat{g}_1$, a unit vector in the $\hat{e}_1$ direction, and gimbal axis $\hat{g}_2$, a unit vector in the $\hat{n}_3$ direction, respectively. All vectors present are expressed in the e basis and superscript R implies that the indicated time differentiation is performed with respect to an observer in the e basis. A detailed derivation of these equations and explanation of the notation employed can be found in Refs. 7 and 9.

To use Eq. (1), the relative acceleration $\ddot{D}_{01}^R$ or relative velocity $\dot{D}_{01}^R$ of the joint with respect to body 0 must be prescribed. Control torques, which appear explicitly in E_0^* and E_1^*, must be specified. To determine the absolute orientation of the vehicles, a set of first order equations, such as the four Euler parameter equations, as well as two trivial equations for determining $\dot{\gamma}_1$ and γ_2 from $\dot{\gamma}_1$ and $\dot{\gamma}_2$, must be added to the system of Eq. (1).

Two additional quantities of interest may be determined using the analysis of Refs. 7 and 9. The constraint torque on body 1 at joint 1, T_{11}^C, is orthogonal to the two axes at the joint about which rotation is allowed, $\hat{g}_1$ and $\hat{g}_2$, and may be shown to be

$$T_{11}^C = (\Phi_{10}+\Phi_{11})\cdot\dot{\omega}_0 + \Phi_{11}\cdot(-\ddot{\gamma}_1\hat{g}_1 + \ddot{\gamma}_2\hat{g}_2)$$
$$-E_1^* - D_{10}\times m[\ddot{D}_{01}^R + 2\omega_0\times\dot{D}_{01}^R] \tag{9}$$

When gravitational effects are neglected, the force acting on body 0 transmitted through joint 1, F_{01}^H, is the only internal force that will act on body 0, that is

$$F_{01}^H = m_0\ddot{r}_0 \tag{10}$$

where r_0 is the vector from the system c.m. to the c.m. of body 0. r_0 may be written as

$$r_0 = (m_1/m)(\mathcal{L}_{10} - \mathcal{L}_{01}) = (m_1/m)\mathcal{L} \tag{11}$$

then

$$F_{01}^H = (m_0m_1/m)[\ddot{\mathcal{L}}^R + 2\omega_0\times\dot{\mathcal{L}}^R + \dot{\omega}_0$$
$$\times\mathcal{L} + \omega_0\times\omega_0\times\mathcal{L}] \tag{12}$$

Equations (9) and (12) provide information on the force and moment that the joint must withstand.

The Optimal Control Problem

The optimal control problem being considered is to drive the OMV-target system from the given initial state to a prescribed final state while minimizing the integral performance index

$$\text{P.I.} = \frac{1}{2}\int_{t_0}^{t_f}\left[\sum_{i=1}^{n} u_i^2\right]dt \tag{13}$$

where u_i represents the system controls. Since there are five rotational degrees of freedom in the two body system, we choose to use five controls, an external torque (i.e., thruster) applied about each of the axes of the e system, and an internal torque applied about each of the two gimbal axes. No control variable is associated with joint translation since the velocity and acceleration profiles are precomputed to satisfy the desired final joint position. It is assumed that the thrusting torques do not change the mass of the OMV.

Using fundamental optimal control theory,[10] the system dynamic and kinematic equations of constraint are adjoined to the integral performance index with Lagrange multipliers or costate variables. After defining the system Hamiltonian, the optimality conditions, by way of the Pontryagin principle, are applied to change the original problem to a two-point-boundary-value-problem (TPBVP) in the state and costate variables. For the most general case of this capture problem, there are 20 independent differential equations defining the TPBVP in terms of 10 independent states and 10 costates.

Formal development of the TPBVP is facilitated by using a more compact form of Eq. (1). We define the 5×5 matrix of Eq. (1) as the matrix A. The five element vector on the right hand side of Eq. (1) is defined as F^*. Finally, we let

$$[\dot{\omega}_{01}\dot{\omega}_{02}\dot{\omega}_{03} - \ddot{\gamma}_1\ddot{\gamma}_2] = [\dot{x}_1\dot{x}_2\dot{x}_3\dot{x}_4\dot{x}_5] = \dot{x} \tag{14}$$

Then Eq. (1) may be written as

$$A\dot{x} = F^* \tag{15}$$

From Eqs.(1) and (7) it is noted that F^* may be decomposed into a sum of two vectors, the control vector u and a vector F consisting of the remaining terms in F^*. Therefore we write

$$A\dot{x} = F + u \tag{16}$$

and finally

$$\dot{x} = A^{-1}F + A^{-1}u \tag{17}$$

where the existence of A^{-1} is guaranteed in this case.

The kinematical equations for γ_1, γ_2, and the Euler parameters complete the formulation of the state equations. The γ_1 and γ_2 equations are respectively

$$\dot{x}_6 = x_4 \tag{18}$$

$$\dot{x}_7 = x_5 \tag{19}$$

The Euler parameter equations in the notation of Junkins and Turner[11] are given as

$$\dot{\beta}=\Omega\beta \tag{20}$$

where

$$\beta^T=[\beta_0\beta_1\beta_2\beta_3] \tag{21}$$

and

$$\Omega=\frac{1}{2}\begin{bmatrix} 0 & -x_1 & -x_2 & -x_3 \\ x_1 & 0 & x_3 & -x_2 \\ x_2 & -x_3 & 0 & x_1 \\ x_3 & x_2 & -x_1 & 0 \end{bmatrix} \tag{22}$$

At this point we have 11 state equations, but as Junkins and Turner[11] point out, only three of the Euler parameter equations are independent since β is constrained by the equation

$$\sum_{i=0}^{3}\beta_i^2=1 \tag{23}$$

The Hamiltonian H for this system is

$$H=\sum_{i=1}^{5}\frac{1}{2}u_i^2+\lambda^T\begin{bmatrix} A^{-1}F+A^{-1}u \\ x_4 \\ x_5 \end{bmatrix}+\nu^T[\Omega\beta] \tag{24}$$

where λ and ν are seven and four element (costate) vectors, respectively. Let

$$\lambda^T=[\Lambda_1^T,\Lambda_2^T] \tag{25}$$

where Λ_1 and Λ_2 are five and two element column vectors, respectively. The necessary condition,

$$H_u=0 \tag{26}$$

gives the optimal control as

$$u^T=-{}_1\lambda_5^TA^{-1}=-\Lambda_1^TA^{-1} \tag{27}$$

meaning that the control vector u is a function of the matrix A and the first elements of the vector λ. Further conditions require that

$$\dot{\lambda}^T=[\dot{\lambda}_1,\dot{\lambda}_2,\dot{\lambda}_3,\dot{\lambda}_4,\dot{\lambda}_5,\dot{\lambda}_6,\dot{\lambda}_7]=-H_x \tag{28}$$

and

$$\dot{\nu}^T=-H_\beta \tag{29}$$

Therefore,

$$\dot{\lambda}^T=-\lambda^T\begin{bmatrix} A^{-1}F+A^{-1}u \\ x_4 \\ x_5 \end{bmatrix}_x-\nu^T[\Omega\beta]_x \tag{30}$$

where x used as a subscript implies differentiation of the indicated, n element column vector with respect to the vector x, yielding an $(n\times 7)$ matrix, and

$$\dot{\nu}^T=-\nu^T\Omega \tag{31}$$

or

$$\dot{\nu}=\Omega\nu \tag{32}$$

since Ω is skew symmetric. Substituting for u in the state Eqs. (17-20) and in the costate Eqs. (30) and (32) gives the system of 22 nonlinear differential equations in the states and costates that form the TPBVP. Junkins and Turner[11] point out, though, that Eqs. (20) and (32) are equivalent and write

$$\sum_{i=1}^{4}\nu_i^2=\text{constant} \tag{33}$$

Therefore, as with β, only three of the equations for ν are independent, so there are, in fact, 20 independent equations in the TPBVP.

Twenty boundary conditions are required to solve the TPBVP with two others determined from Eqs. (23) and (33). The 11 state variables are generally specified at the initial time t_0 and some or all of them specified at the final time t_f. For those state variables unspecified at t_f, their associated costate variables must be zero at t_f, except where Eq. (33) must hold,[12] since the performance index is not a function of the final state.

Solving this TPBVP numerically is a very formidable task. While Junkins and Turner[11] have treated the optimal control of a rigid body with 12 independent equtions forming the TPBVP, moving forward to treat systems of rigid bodies is not a trivial step. Even with a two-body system, the state equations are much more complex, and the costate equations become equally so. The two dependent equations, as pointed out by Junkins and Turner,[11] also require special treatment. The dimensionality increase has obvious impacts on computer storage requirements. Therefore, as a first attempt at solving this type of problem, its dimension should be reduced without eliminating all reasonable solutions.

The effect of gravity-gradient torques has been deliberately ignored. The state Eqs. (1) or (16) then become independent of vehicle attitude. If in addition the final attitude of the OMV, $\beta(t_f)$, is unspecified, there is a simple, analytic solution for the attitude costates, $\nu(t)=0$. In fact, this solution for ν is not unique, but all admissible solutions will yield the same angular rate costate history, $\lambda(t)$, and hence the same optimal control $u(t)$.[11] This occurs because all admissible variations to the original admissible costate history $\nu(t)$ are such as to yield no change in the system Hamiltonian, Eq. (25).[12] Therefore, if the attitude of the OMV is not to be controlled, it is not necessary to integrate the differential equations for ν and β to determine the optimal control. The attitude equations [Eq. (20)] may of course be integrated a posteriori if the attitude history is of interest.

Leaving the final value of x_7 unspecified yields a similar result. The symmetry of the target makes the Hamiltonian independent of x_7 which yields

$$\dot{\lambda}_7=0 \tag{34}$$

and

$$\lambda_7=\text{constant} \tag{35}$$

But $\lambda_7(t_f)$ is zero since $x_7(t_f)$ is free; therefore, $\lambda_7(t)$ is zero.

The TPBVP is now reduced to a system of 12 independent equations in six state and six costate variables, which is summarized as follows:

$$\dot{x}=A^{-1}F+A^{-1}u \tag{36}$$

$$\dot{x}_6=x_4 \tag{37}$$

$$ {}_1\dot{\lambda}_6 = -{}_1\lambda_6^T \begin{bmatrix} A^{-1}F + A^{-1}u \\ x_4 \end{bmatrix}_{1x_6} \tag{38} $$

where Eq. (27) is used to substitute for u after the indicated partial differentiation is performed. The meaning of the double subscript notation, applied to a vector, should be clear from its use in Eqs. (25) and (27). The state boundary conditions we shall consider are summarized in Table 2.

Allowing ω_{03} to be free at t_f requires that $\lambda_3(t_f)$ be zero, giving the twelfth boundary condition required to solve the TPBVP.

Having reduced the TPBVP to this form, the solution is obtained by a discretization method using a Newton iteration. The algorithm is based on the method developed by Pereyra[13] and requires the Jacobian matrix, given in Eq. (39), to be nonsingular to compute the Newton corrections.

$$ J = \begin{bmatrix} \frac{\partial \dot{x}}{\partial x} & \frac{\partial \dot{x}}{\partial \lambda} \\ \frac{\partial \dot{\lambda}}{\partial x} & \frac{\partial \dot{\lambda}}{\partial \lambda} \end{bmatrix} \tag{39} $$

Computer storage requirements are manageable, and single precision computations are adequate for reasonable accuracy.

Great care in deriving and coding the Jacobian matrix is essential. We were able to derive analytical expressions for all but one element of the matrix, and these were verified at a selected point in the state and costate space by using a numerical differentiation technique. Agreement to at least eight places was always achieved. The complexity of the last partial derivative $\partial\dot{\lambda}_6/\partial\gamma_1$ and the accuracy achieved above led to using the numerical method for this one derivative to complete the Jacobian.

The results of a successful run of the algorithm are in the form of a grid. The differential equations are discretized and solved at program selected points between t_0 and t_f, so the solution grid contains the converged values of the states and costates at those same points. The control grid can then be computed using Eq. (27). Equations (9) and (12) may also be applied over the grid to solve for the histories of the constraint torque and constraint force on the joint.

To this point, a method has been developed by which continuous optimal open loop controls that solve the capture problem can be found. Continuously variable thrusters are, however, an idealization, so the advantages of simplifying the control system by way of control constraints at the expense of increasing the cost of the capture is examined. One realistic control constraint is to require the thruster torques about the axes of the e system to be constants during the capture. A second constraint considered is to require the torque about gimbal axis one to be proportional to the angle γ_1 and the angular rate $\dot{\gamma}_1$, representing torsional spring and damper.

The method of adjoining these control constraints to the problem is described in Ref. 10. In the case of constant thruster torques Eq. (25) for the Hamiltonian becomes

$$ H = \sum_{i=1}^{5} \frac{1}{2} u_i^2 + \lambda^T \begin{bmatrix} A^{-1}F + A^{-1}u \\ x_4 \\ x_5 \end{bmatrix} + \nu^T[\Omega\beta] + \mu^T[{}_1u_3 - {}_1c_3] \tag{40} $$

where μ is a three element vector of Lagrange multipliers. The same necessary conditions apply; they are Eqs. (26), (28), and (29). The TPBVP reduces to a system of 12 differential equations as before, and the required changes to the Jacobian matrix are straightforward. Note that the $\dot{\lambda}$ equations do not change with the addition of these constraints. In the second case μ becomes a scalar and the control constraint is

$$ u_4 - k_1\gamma_1 - k_2\dot{\gamma}_1 = 0 \tag{41} $$

Now $\dot{\lambda}_4$ and $\dot{\lambda}_6$ are functions of μ, so the adjustments to the Jacobian are slightly more involved. Again, the dimension of the problem remains at 12. For comparison purposes, the initial and final conditions of Table 2 are also used to solve the constrained control problems.

Results

The results presented are for a system with the mass properties and initial conditions of Tables 1 and 3. The final time is chosen to be 300 seconds. The joint translational velocity is chosen to move the joint to the center in that time and is assumed constant. Solution accuracy is controlled by setting the relative error tolerance used by the algorithm to the desired level: 1.0×10^{-6} for all cases. A simple linear problem was solved first and checked against the analytical solution to verify the computer code. When referring to the figures that follow note that

$$ [\omega_{01},\omega_{02},\omega_{03},\dot{\gamma}_1,\dot{\gamma}_2,\gamma_1,u_1,u_2,u_3,u_4,u_5] = [W1,W2,W3,G1D,G2D,G1,T1,T2,T3,TG1,TG2] $$

In case 1 all five controls are unconstrained. Figures 2-7 summarize the histories of the states, controls, and the internal constraint force and torque. Eighty-seven grid points were required to achieve this solution. The minimum value of the performance index was computed to be 2.335. Figure 2 indicates that the angular velocity vector of the OMV remains very nearly aligned with the body fixed $\hat{e}_3$ axis during capture. The nearly constant behavior of ω_{03} in Fig. 2 is the result of scaling. Small fluctuations in ω_{03} can be seen in the actual output, and at 300 s, ω_{03} is -0.101 rad/s. Figure 3 shows the smooth behavior of γ_1 and $\dot{\gamma}_2$ in decreasing from their initial values to zero at 300 s. Figure 4 shows that $\dot{\gamma}_1$ remains very small during capture and, along with Fig. 2, suggests that optimal capture should be quite a benign process. By showing the external and internal control torques, Figs. 5 and 6 are encouraging in that the magnitudes of all controls appear not to

Table 2 State boundary conditions

	t_0	t_f
ω_0	0.0	0.0
ω_{02}	0.0	0.0
ω_{03}	specified	free
$\dot{\gamma}_1$	0.0	0.0
$\dot{\gamma}_2$	specified	0.0
γ_1	specified	0.0

Table 3 Initial conditions

	ω_{01}	0.0
	ω_{02}	0.0
	ω_{03}	-0.102 rad/s
	$\dot{\gamma}_1$	0.0
	$\dot{\gamma}_2$	-0.009 rad/s
	γ_1	0.349 rad
Initial joint position	$\mathcal{L}_{01}$	(0.0 m) $\hat{e}_1$ + (-0.599 m) $\hat{e}_2$ + (0.62 m) $\hat{e}_3$
Joint velocity		(0.002 m/s) $\hat{e}_2$
Joint acceleration		0.0 m/s^2
Length (constant)	$\mathcal{L}_{10}$	(1.75 m) $\hat{n}_3$

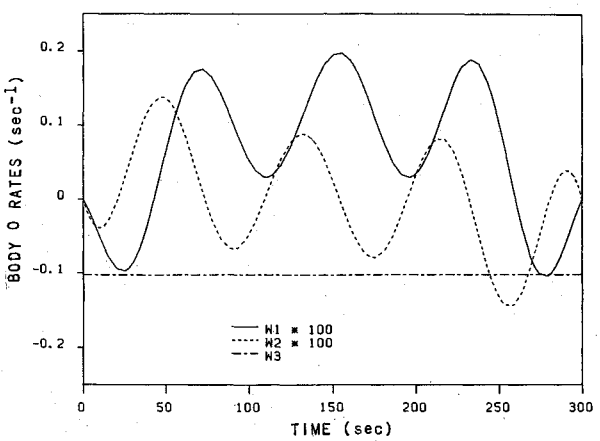

Fig. 2 Body 0 angular rate history: case 1.

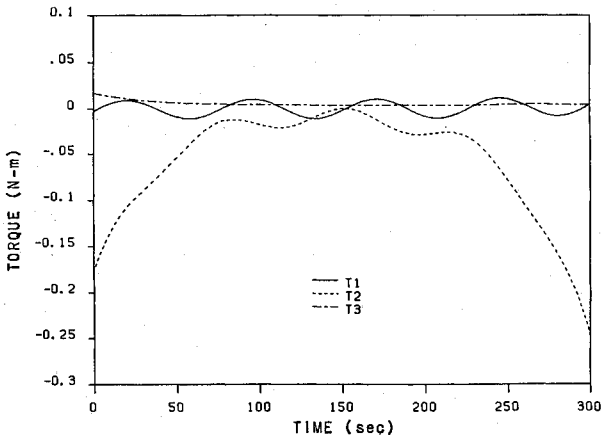

Fig. 5 External (thruster) torque history: case 1.

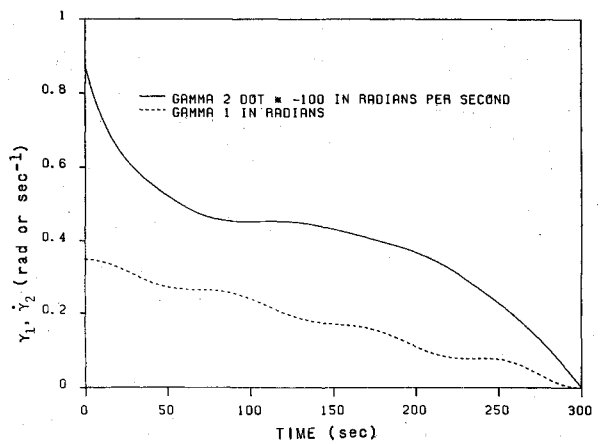

Fig. 3 Body 1 relative motion history: case 1.

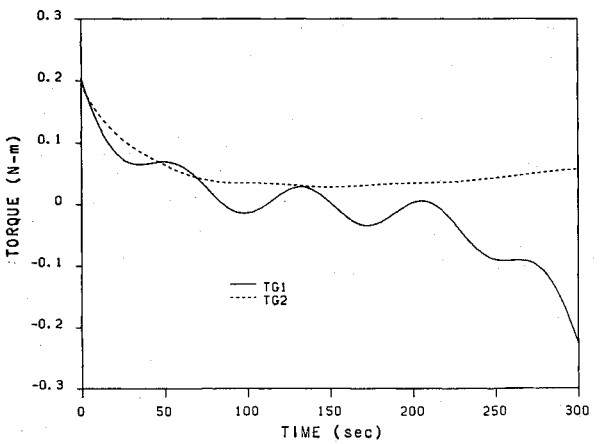

Fig. 6 Internal (joint) torque history: case 1.

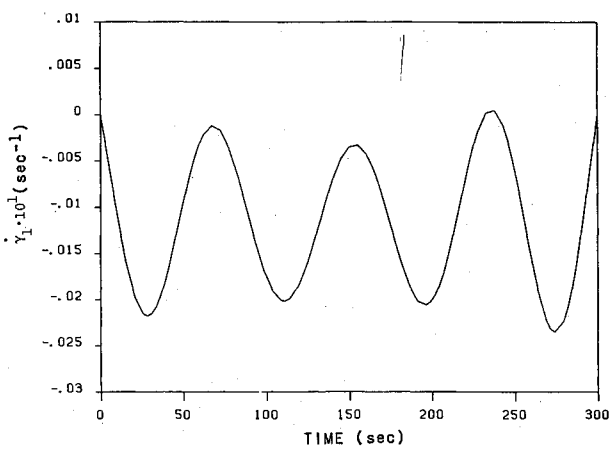

Fig. 4 Body 1 relative angular rate history: case 1.

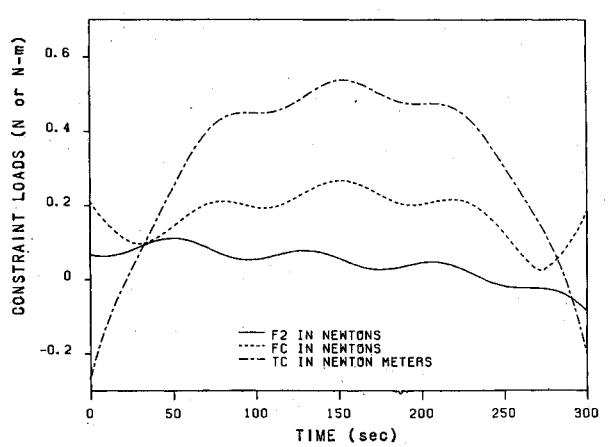

Fig. 7 Constraint load history: case 1.

impose excessive requirements on the control system or to require much longer time intervals for capture. In Fig. 7, FC is the magnitude of the constraint force on the joint, and TC is the dot product of the joint constraint torque with the constraint axis, which forms a dextral set with $\hat{g}_1$ and $\hat{g}_2$. Figure 7 indicates that the constraint loads on the joint should not require a prohibitively massive or stiff structure to link the OMV and target. Also in Fig. 7 the component of FC in the $\hat{e}_2$ direction, $F2$, is the force required to maintain the constant joint velocity during capture and also appears to pose no excessive control requirement.

Case 2 considers the external torques, $T1$, $T2$, and $T3$, to be constant during capture. Their assigned values are $T1 = 0.0$, $T2 = -0.07$, and $T3 = 0.011$ Nm. The final grid size remained at 87, and the performance index was computed to be 3.066. Except for the external torques, the corresponding figures of case 2 are not significantly different from those of case 1 so are not presented here. The increase in the performance index is the only immediate quantitative difference between the two cases. Of significance is the fact that capture is possible with one component of the torque set to zero. This raises the question of what minimum control configuration is required from controllability considerations.

In case 3 the internal torque, $TG1$, is assumed to be produced by a torsional spring and damper. $TG1 = u_4 = .57\gamma_1 + 100\dot{\gamma}_1$ is chosen as the torque constraint. The final grid

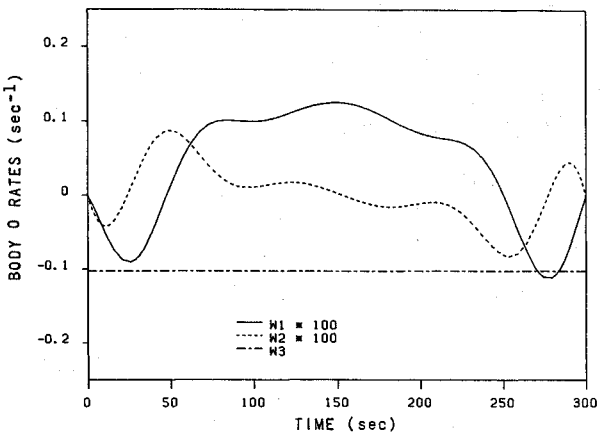

Fig. 8 Body 0 angular rate history: case 3.

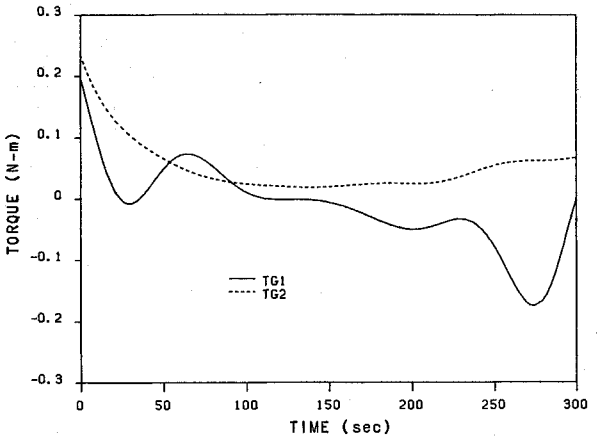

Fig. 11 Internal (joint) torque history: case 3.

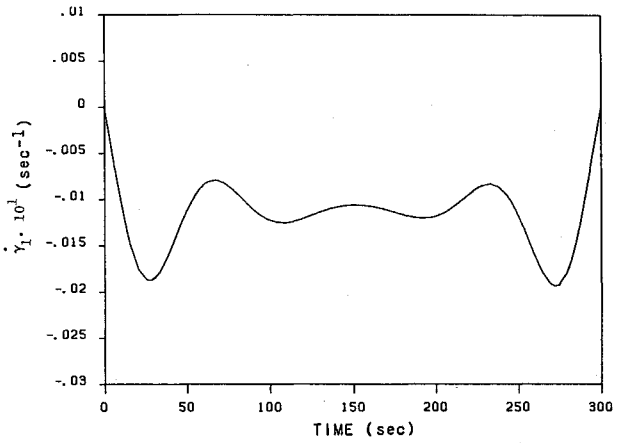

Fig. 9 Body 1 relative angular rate history: case 3.

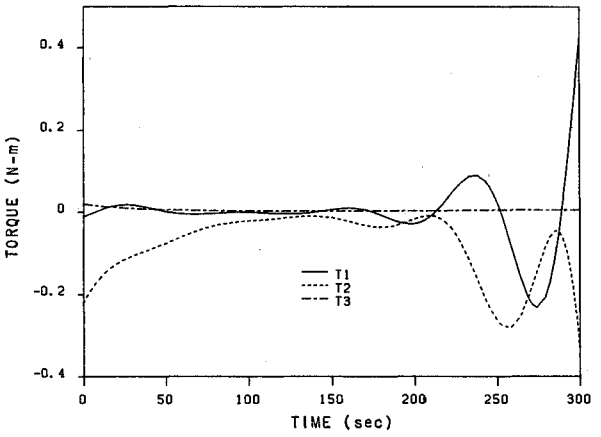

Fig. 10 External (thruster) torque history: case 3.

size was again 87, and the performace index 4.108. The constraint loads and the behavior of γ_1 and $\dot{\gamma}_2$ were not significantly different from those of case 1, so their figures are omitted here. Figures 8 through 11 can be compared to the results of case 1 to see more significant changes in the motion and torque histories. As *TG*1 goes to zero at 300 s, the magnitudes of *T*1 and *T*2 increase significantly to achieve the specified final state. Other constants in the torque constraint might yield lower cost.

Conclusions

We believe that we have presented a more realistic approach to the problem of remote orbital capture than those previously attempted. By treating the coupled dynamics of an orbital maneuvering vehicle-target system with translational motion in the connecting joint, continuous controls have been produced that accomplished a very benign detumbling with no significant change in the attitude of the spinning retriever. Only very moderate internal (joint) and external (thruster) torque magnitudes are required for a very reasonable maneuver time of 300 s. Two examples have been presented of the effect of control constraints of the type that are likely to be imposed on a real vehicle. Our results should serve to provide a more realistic model of the capture problem and help to size the structural and control requirements of a retriever spacecraft.

References

[1]Onega, G.T. and Clingman, J.H., "Free-Flying Teleoperator Requirements and Conceptual Design," *Proceedings of the First National Conference on Remotely Manned Systems,* edited by E. Heer, California Institute of Technology, Pasadena, CA, 1973, pp. 19-32.

[2]Smith, G.W. and DeRocher, W.L., "Orbital Servicing and Remotely Manned Systems," *Mechanism and Machine Theory,* Vol. 12, 1977, p. 65-76.

[3]Faile, G.C., Counter, D.N., and Bourgeois, E.J., "Dynamic Passivation of a Spinning and Tumbling Satellite Using Free-Flying Teleoperators," *Proceedings of the First National Conference on Remotely Manned Systems,* edited by E. Heer, California Institute of Technology, Pasadena, CA, 1973, pp. 63-73.

[4]Kaplan, M.H. and Nadkarni, A.A., "Control and Stability Problems of Remote Orbital Capture," *Mechanism and Machine Theory,* Vol. 12, 1977, pp. 57-64.

[5]Conway, B.A., Tuliglowski, J.E., and Webber, P.D., "Dynamics of Remote Orbital Capture," *Proceedings of the AAS/AIAA Astrodynamics Specialist Conference,* Lake Placid, NY, 1983.

[6]Hooker, W.W. and Margulies, M., "The Dynamical Attitude Equations for an N-Body Satellite," *Journal of the Astronautical Sciences,* Vol. 12, Winter 1965, pp. 123-128.

[7]Hooker, W.W., "A Set of *r* Dynamical Attitude Equations for an Arbitrary N-Body Satellite Having *r* Rotational Degrees of Freedom," *AIAA Journal,* Vol. 8, July 1970, pp. 1205-1207.

[8]Greenwood, D.T., *Principles of Dynamics,* Prentice-Hall, Inc., Englewood Cliffs, NJ, 1965, pp. 383-391.

[9]Conway, B.A. and Widhalm, J.W., "Equations of Attitude Motion for an N-Body Satellite with Moving Joints," *Journal of Guidance, Control, and Dynamics,* July-Aug. 1985, pp. 537-539.

[10]Bryson, A.E., Jr. and Ho, Y., *Applied Optimal Control,* Ginn and Co., Waltham, MA, 1969, Chaps. 2 and 3.

[11]Junkins, J.L. and Turner, J.D., "Optimal Continuous Torque Attitude Maneuvers," *Journal of Guidance and Control,* Vol. 3, May-June 1980, pp. 210-217.

[12]Vadali, S.R., Kraige, L.G., and Junkins, J.L., "New Results on the Optimal Spacecraft Attitude Maneuver Problem," *Journal of Guidance, Control, and Dynamics,* Vol. 7, May-June 1984, pp. 378-380.

[13]Pereyra, A., "PASVA3: An Adaptive Finite Difference FORTRAN Program for First Order Nonlinear Ordinary Boundary Problems," *Lecture Notes in Computer Science,* Vol. 76, Springer-Verlag, Berlin, 1978, pp. 67-88.